Data Delivery Properties of Human Contact Networks

Nishanth Sastry, *Member, IEEE,* D. Manjunath, *Member, IEEE,* Karen Sollins, *Member, IEEE,* and Jon Crowcroft, *Fellow, IEEE*

Abstract—Pocket Switched Networks take advantage of social contacts to opportunistically create data paths over time. This work employs empirical traces to examine the effect of the human contact process on data delivery in such networks. The contact occurrence distribution is found to be highly uneven: contacts between a few node pairs occur too frequently, leading to inadequate mixing in the network, while the majority of contacts occur rarely, but are essential for global connectivity. This distribution of contacts leads to a significant variation in the fraction of node pairs that can be connected over time windows of similar duration. Good time windows tend to have a large clique of nodes that can all reach each other. It is shown that the clustering co-efficient of the contact graph over a time window is a good predictor of achievable connectivity. We then examine all successful paths found by flooding and show that though delivery times vary widely, randomly sampling a small number of paths between each source and destination is sufficient to yield a delivery time distribution close to that of flooding over all paths. This result suggests that the rate at which the network can deliver data is remarkably robust to path failures.

Index Terms—Pocket Switched Networks, human mobility networks, flooding, statistical properties, path failure tolerance

THE Pocket Switched Network (PSN) [1] proposes to ferry data using human social contacts. At each contact opportunity, mobile devices carried by the humans exchange data using short-range protocols such as bluetooth or Wi-Fi. By chaining such contacts, the PSN opportunistically creates data paths that connect a source and destination *over time*. Intermediate nodes in the path store data on behalf of the sender and carry it to the next contact opportunity where it is forwarded further.

Although this store-carry-forward network can incur long and highly variable delays, it has the advantage of not requiring infrastructure setup or maintenance. It is therefore useful when infrastructure is damaged (e.g. after disasters), or does not exist (e.g. in remote areas). Also, mobility increases network capacity at the expense of delays, providing multi-user diversity gains [2]. A PSN can be effective as a multi-hop "sneakernet" for high-bandwidth applications that can tolerate delays.

A central question for the success of this approach is to understand how human contact occurrences shape data delivery. In this paper, we explore this issue using empirical traces of human contacts. Our simulations discover the quickest paths by flooding data at every contact opportunity. We then study the achievable performance of the contact network in terms of the fraction of data delivered (delivery ratio), as well as the time to delivery.

The delivery ratio at the end of a time window is indicative of the fraction of node pairs connected during the window and is therefore a measure of the connectivity achieved by the network. The empirically observed cumulative distribution of delivery times can also be interpreted as the evolution in time of delivery ratio, normalised by the ratio eventually achieved at the end of the time window[1], and thus represents the rate at which connectivity is achieved.

To explain our findings, consider an abstract model of the PSN as a temporally evolving contact graph. Each contact corresponds to a momentary undirected edge and involves a two-way data exchange between the node pair involved. Edges appear and disappear according to some underlying stochastic process that corresponds to the social contacts. The sequences of edges (contacts) that occur constitutes a trace of the PSN.

An empirical *contact occurrence distribution* can be defined for a trace, as the probability $p(f)$ that an edge (contact) constitutes a fraction f of the trace[2]. By constructing synthetic and time-shuffled traces from the original, we show that delivery ratio evolves similarly when the contact occurrence distribution is the same.

We then study how this distribution affects delivery ratio in our empirical traces and find the distribution to be highly skewed: Most node pairs meet rarely (fewer than ten times), whereas a few node pairs meet much more frequently (hundreds of times). The PSN's ability to connect two nodes over time depends crucially on the rare contacts. In contrast, frequent contacts often occur

- *N. Sastry and J. Crowcroft are with the University of Cambridge, UK. E-mail: Firstname.Lastname@cl.cam.ac.uk*
- *D. Manjunath is with Indian Institute of Technology Bombay, India. E-mail: dmanju@ee.iitb.ac.in*
- *K. Sollins is with Masachusetts Institute of Technology, USA. E-mail: sollins@csail.mit.edu*

1. If the empirical probability that the delivery time is less than t is r, then a fraction r of the data that eventually get delivered have been delivered by time t.

2. i.e., the nodes that form the edge contact each other fn times in a time window with n contacts.

without there being new data to exchange, even when flooding is the route selection strategy used. This inadequate intermingling of contacts increases the number of contacts needed to achieve a given delivery ratio.

While it would appear from this macroscopic picture that PSNs are largely inefficient, we find that over time windows of fixed duration, there is a significant variation in the achieved delivery ratio. We discover that in time windows in which a large fraction of data gets delivered, rather than all nodes being able to uniformly reach each other with the same efficiency, there is usually a large *clique* of nodes that have 100% reachability among themselves. We show how to identify such time windows and the nodes involved in the clique by computing a clustering co-efficient on the contact graph.

Finally, we examine the effect of path failures on data delivery. Flooding finds a number of paths between each source and destination. Unless all these paths fail, data will eventually be delivered. However, since there is a wide variation in the delivery time distributions of the quickest and slowest paths between node-pairs, time to delivery is expected to increase if some of the quicker paths fail. To understand this, we examine the impact of failing a randomly chosen subset of the paths found by flooding between each sender and destination and find that the delivery time distribution is remarkably resilient to path failures.

Specifically, we study two failure modes among paths found by flooding: The first, proportional flooding, examines delivery times when only a fixed fraction μ of paths between a sender and destination can be used. The second, k-copy flooding, assumes that at most a fixed number $k > 1$ of the paths between a node-pair survive. In both cases, we find that the delivery time distribution of the quickest paths can be closely approximated with relatively small μ and k. It is shown that a constant increase in μ (respectively, k) brings the delivery time distribution of proportional (k-copy) flooding exponentially closer to the delivery time distribution of the quickest paths found by flooding.

Since the delivery time distribution can be seen as the rate of delivery ratio evolution, the above indicates that the rate at which connectivity is achieved is not greatly affected even if many of the paths fail for one reason or another. The success of $k > 1$-copy flooding can also provide a loose motivation for heuristics-based routing algorithms that explore multiple paths simultaneously.

The rest of the paper is structured as follows: Sec. 1 presents the details of our simulations and motivates our methodology. Sec. 2 discusses the effect of the order and distribution of contact occurrences on data deliveries. Sec. 3 shows how to exploit periods of good connectivity by identifying cliques of nodes which can all reach each other. Next we explore the time evolution of delivery ratio by studying the delivery time distribution: In Sec. 4 we discuss components that contribute to delay on successful paths and Sec. 5 shows that random sampling closely approximates the quickest possible delivery times. Sec. 6 discusses related work and Sec. 7 concludes.

1 Setup and Methodology

This section motivates the choice of traces, the simulation setup and the performance measures used.

1.1 Traces

We imagine the participants of a PSN would be a finite group of people who are at least loosely bound together by some context—for instance, first responders at a disaster situation, who need to send data to each other. Multiple PSNs could co-exist for different contexts, and a single individual could conceivably participate in several different PSNs[3].

Our model that PSN participants form a cohesive group places the requirement that an ideal PSN should be able to create paths between arbitrary source-destination pairs. This is reflected in our simulation setup, where the destinations for each source node are chosen randomly. Also, our traces are picked to be close to the limits of Dunbar's number (=147.8, 95% confidence limits: 100.2–231.1), the average size for cohesive groups of humans [4].

The first trace comes from a four week subset of the UCSD Wireless Topology Discovery [5] project which recorded Wi-Fi Access Points seen by subjects' PDAs. We treat PDAs simultaneously in range of the same Wi-Fi access point as a contact opportunity. This data has $N = 202$ subjects. The second trace consists of bluetooth contacts recorded from 1 Nov. 2004 to 1 Jan. 2005 between participants of the MIT Reality Mining project [6]. We conservatively set five minutes as the minimum allowed data transfer opportunity and discarded contacts of durations smaller than this cutoff. This trace has contacts between $N = 91$ subjects.

The subjects in the MIT trace consist of a mixture of students and faculty at the MIT Media Lab, and incoming freshmen at the MIT Sloan Business School. The UCSD trace is comprised of a select group of freshmen, all from UCSD's Sixth College. As such, we can expect subjects in both traces to have reasons for some amount of interaction, leading to a loosely cohesive group structure. Prior work on community mining using the same traces supports this [7].

It is important to emphasize that our focus is solely on the capability and efficiency of the human contact process in forming end-to-end paths. The precise choice of the minimum data transfer opportunity is less important—it is entirely possible that a new technology would allow for faster node-node transfers. Indeed, our results are qualitatively similar for other cutoff values tested. Similarly, a different technology for local node-node transfers could have different "reach," allowing

3. Note that this is in contrast to a single unboundedly large network of socially unrelated individuals as in the famous "small-world" experiment [3] that examined a network essentially comprising all Americans and discovered an average 5.2 (≈ 6) degrees of separation.

more nodes to be in contact with each other simultaneously. Nevertheless, the substantial similarities (see rest of the paper) between results based on two different technologies and traces—the Wi-Fi based UCSD trace and the bluetooth based MIT trace—gives us some confidence that the results below may be applicable beyond the traces and technologies we have considered.

1.2 Simulation setup and measurement

Setup: At the beginning of simulation, data is created, marked for a randomly chosen destination, and associated with the source node. An oracle with complete knowledge of the future can choose to transfer data at appropriate contact opportunities and thereby form the quickest path to the destination. To simulate this, we enumerate all possible paths found by flooding data at each contact opportunity, and choose the quickest.

Performance measure: Consider the time-ordered sequence (with ties broken arbitrarily) of contacts that occur globally in the network. Since there are $N(N-1)$ quickest paths between different sender-destination pairs, a maximum[4] of $N(N-1)$ contacts in the the global sequence of contacts act as path completion points. Of these, Nd become "interesting" when there are d destinations per sender. Since the destinations are chosen randomly, we might expect that on average, if k path completion points have occured, the *fraction* of these that are interesting is independent of d: When d is greater, more data gets delivered after k path completion points, but there is also more data to deliver.

The above discussion motivates our method of measuring the efficiency of the PSN: At any point in the simulation, the *delivery ratio*, measured as the fraction of data that has been delivered, or equivalently, the number of "interesting" path completion points we have seen, is taken as a figure of merit. The more efficient the PSN is, the faster the delivery ratio evolves to 1, as the number of contacts and time increase.

Unless otherwise specified, our experiments examine delivery ratio evolution statistically averaged over 10 independent runs, with each run starting at a random point in the trace, and lasting for 6000 contacts. We confirm our intuition in Fig. 1, which shows that the delivery ratio evolves similarly, whether d is 1 or a maximum of $N-1$ destinations per sender. We note that the graph also represents the fastest possible evolution of the delivery ratio under the given set of contacts, due to the use of flooding.

2 Order and Distribution of Contacts

A PSN contact trace is determined by the distribution of contact occurrences and the time order in which these contacts occur. In this section, we examine how these properties affect delivery ratio evolution.

4. The actual number could be lesser because a contact with a rarely active node could complete multiple paths that end in that node.

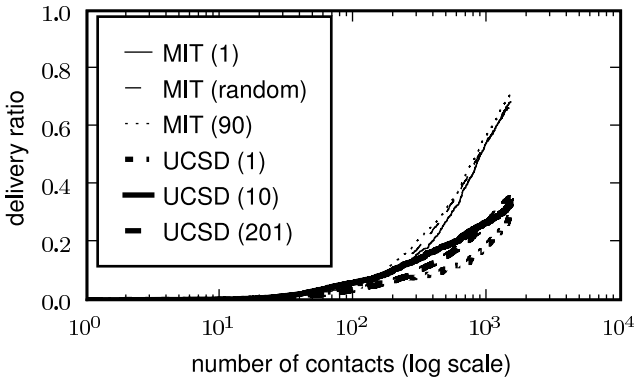

Fig. 1. Fraction of data delivered as a function of the number of contacts, for the MIT and UCSD traces (number of destinations per sender shown in brackets). The curves for each network are clustered together, showing that the delivery ratio evolves independently of the load.

Given two traces, the more efficient one will manage to achieve a given delivery ratio with fewer number of contacts. Our approach is to create a synthetic trace from the original trace by disrupting the property we wish to study. Comparing delivery ratio evolution in the original and synthetic traces informs us about the effects of the property.

Our main findings are that in both the traces we examine, time correlations between contacts that occur too frequently leads to non-effective contacts in which no new data can be exchanged, and that the progress of the delivery ratio as well as the connectivity of the PSN itself are precariously dependent on rare contacts.

2.1 Frequent contacts are often non-effective

To investigate the effect of the time order in which contacts occur, we replay the trace, randomly shuffling the time order in which links occur. Observe in Fig. 2 that the curve marked "shuffled" evolves faster than "trace" implying that the delivery ratio increases faster after random shuffling. The random shuffle has the effect of removing any time correlations of contacts in the original trace. Thus the improved delivery ratio evolution implies that time correlations of the contacts in the original data slowed down the exchange of data among the nodes, causing them to be delivered later.

Manual examination reveals several time correlated contacts where two nodes see each other multiple times without seeing other nodes. At their first contact, one or both nodes could have data that the other does not, which is then shared by flooding. After this initial flooding, both nodes contain the same data—subsequent contacts are "non-effective", and only increase the number of contacts happening in the network without increasing the delivery ratio.

To quantify the impact, in the curve marked "effective" on Fig. 2, we plot delivery ratio evolution in the original trace, counting only the contacts in which data

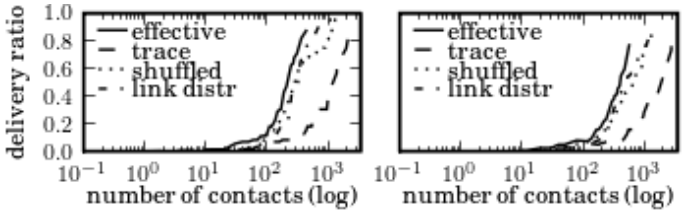

Fig. 2. Delivery ratio evolution for synthetically derived variants of MIT (left), UCSD (right) traces. 'Trace' is the original. 'Shuffled', the same trace with time order of contacts randomly shuffled. 'Effective' replays 'trace', counting only contacts where data was exchanged. 'Link distr' is an artificial trace with the same size and contact occurrence distribution as the original.

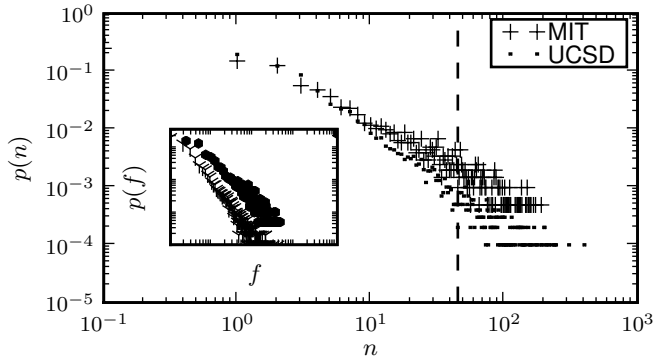

Fig. 3. Contact occurrence distributions (log-log): A random edge appears n times with probability $p(n)$. To the left of the dashed line at $n = 45$, the distributions for both traces coincidentally happen to be similar. The inset shows the difference when normalised by the number of contacts in the trace. In the inset, a random edge constitutes a fraction f of the trace with probability $p(f)$.

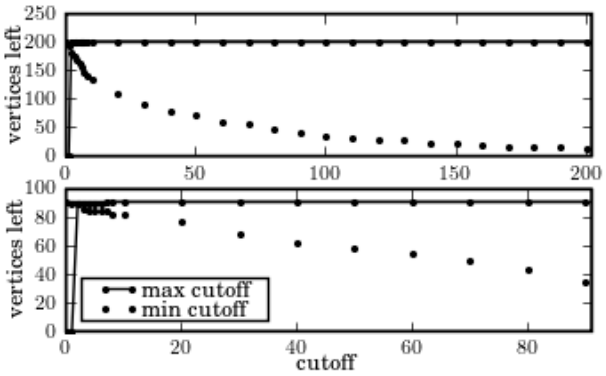

(a) Robustness to cutoff: MIT (below), UCSD (above). Max cutoff specifies a maximum cutoff for the frequency of contacts, thus removing the most frequently occurring ones. Min cutoff specifies a minimum frequency of contacts—removing the rarest contacts causes the number of nodes that are connected to drop precipitously.

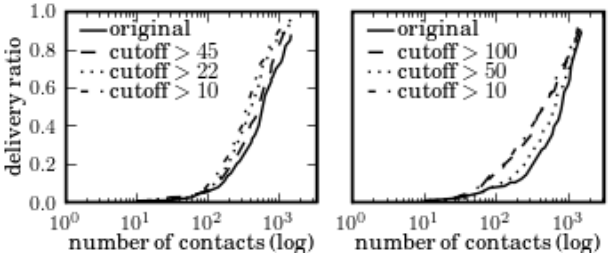

(b) Evolution of delivery ratio with contacts that occur more than `cutoff` times removed. MIT (left), UCSD (right). The network still remains connected, and manages to deliver data with *fewer* contacts.

Fig. 4. Relative importance of rare and frequent contacts

could be exchanged. This coincides well with the time-shuffled trace, showing that non-effective contacts are largely responsible for the slower delivery ratio evolution in the original trace.

Next, we construct a synthetic trace that has the same number of nodes as the original trace, as well as the same contact occurrence distribution. By this, we mean that the probability of contact between any pair of nodes is the same as in the original trace. The delivery ratio evolution of this trace, depicted as "link distr" in Fig. 2, is seen to evolve in a similar fashion as the time-shuffled trace. This indicates that once time correlations are removed, the delivery properties are determined mainly by the contact occurrence distribution.

2.2 Connectivity depends on rare contacts

The fact that three different traces (shuffled, effective, and link distr), which are based on the same contact occurrence distribution, essentially evolve in the same manner leads us to examine this distribution further.

Fig. 3 shows that the contact occurrence distribution has both highly rare contacts (involving node pairs that meet fewer than ten times in the trace) as well as frequent contacts (nodes which meet hundreds of times). A randomly chosen contact from the trace is much more likely to be a rare contact than a frequent one.

Fig. 4a shows that the rare contacts are extremely important for the nodes to stay connected. When contacts that occur fewer than a minimum cutoff number of times are removed, the number of nodes remaining in the trace falls sharply. This implies that there are a number of nodes which are connected to the rest of the nodes by only a few rare contacts.

On the other hand, removing the frequent contacts (by removing contacts occuring more than a maximum cutoff number of times) does not affect connectivity greatly. For instance, the MIT trace remains connected even when the maximum cutoff is as low as 10 (i.e., contacts occurring more than ten times are removed). This suggests that nodes which contact each other very frequently are also connected by other paths, comprising only rare edges.

Interestingly, Fig. 4b shows that with the most frequent edges removed, achieving a given delivery ratio can

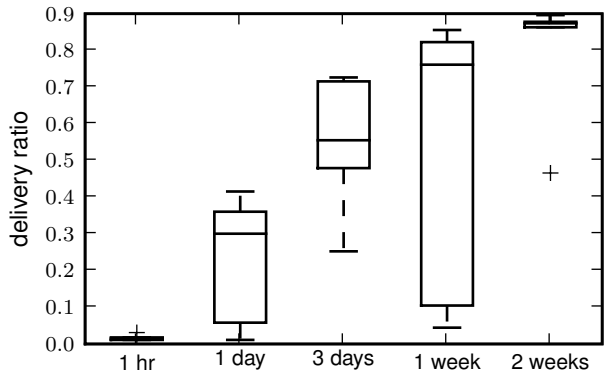

Fig. 5. Distribution of delivery ratios over different time windows (MIT). Allowing more time generally results in more delivery, but there is significant variation. Each box extends from the lower to upper quartile values, with a line at the median. Whiskers extend from the box to show the range. Outliers past the whiskers are plotted individually.

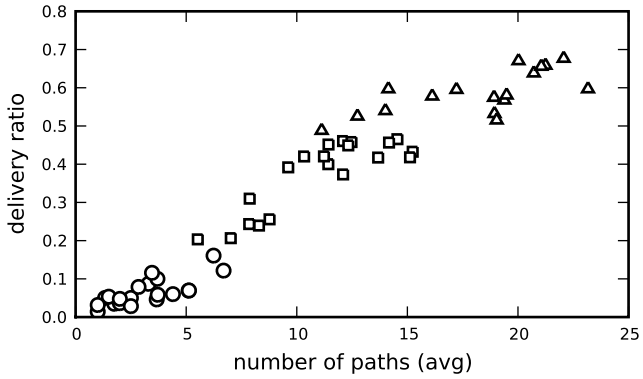

Fig. 6. Scatter plot showing a correlation between delivery ratio during random time windows of different sizes and the mean number of paths connecting node pairs. Squares, circles and triangles represent windows of one-hour, one-day and 3 days, respectively (UCSD trace).

take fewer contacts. This appears paradoxical but can be explained as follows: In terms of time, data delayed waiting for the occurrence of a rare contact still take the same amount of time to reach the destination, and data previously sent on paths containing more frequent edges alone are delayed, because they now have to be re-routed over rare contacts. However, the reliance on rare contacts allows "batch-processing": Each node involved in the rare contact has more data to exchange when the contact happens, thus decreasing the overall *count* of contacts taken to achieve a given delivery ratio.

3 Delivery over fixed duration windows

The previous section showed that at a macroscopic level, a PSN is a challenged network, with connectivity crucially dependent on rare contacts, and frequent contacts non-effective for data transfer. This section examines time windows of fixed duration. It is observed that there can be a large variation in the delivery ratio achieved between windows of same duration. Time windows which achieve a high delivery ratio are characterised by unequal connectivity, with a large clique of nodes having 100% connectivity amongst themselves and much worse connectivity among the other nodes.

Fig. 5 shows the distribution of delivery ratios achieved by flooding data between every possible source-destination pair over time windows of different sizes. On average, allowing more time increases the delivery ratio. This is expected because the number of contacts can only increase over time. However, there is still significant variation, especially within windows of shorter duration, and the distributions are clearly skewed (observe the positions of the median).

3.1 Large cliques correlate with good connectivity

Over fixed time windows, the temporal contact graph of the PSN can be viewed as constructing a *static* reachability graph where a directed edge is drawn from node s to t if the sender s can transfer data to destination t during that window. The reachability graph is constructed by flooding data during the window between every possible source-destination pair. We examine this graph for clues about successful time windows which achieve high delivery ratios.

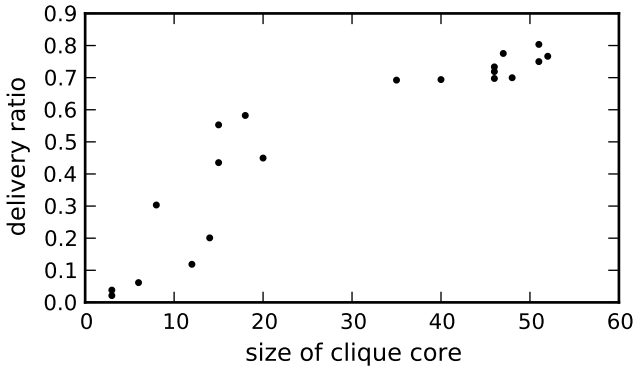

Fig. 7. Delivery ratio in the contact graph correlates with size of maximum clique observed in the reachability graph (MIT trace, non-overlapping 3-day windows).

A preliminary examination (Fig. 6) shows that the average number of paths connecting a source and destination in the contact graph in the UCSD trace exhibits a significant correlation with the achieved delivery ratio. A similar result can be obtained for the MIT trace.

To uncover the reason, we focus on the MIT trace and divide the entire duration of the trace into non-overlapping 3-day windows and examine the reachability graph of each window for subsets of nodes with large numbers of paths. We find that windows with high delivery ratio tend to have a large subset of nodes that form a clique in the reachability graph (Fig. 7). By definition, each member of a clique in the reachability graph can reach every other member of the clique,

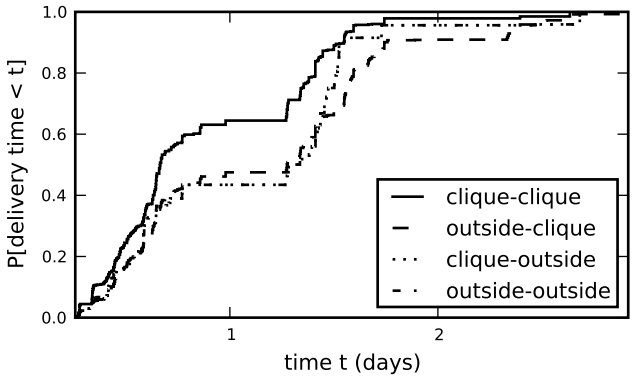

Fig. 8. CDFs of delivery times during a 3-day window with a 46 node clique. The four categories shown are different combinations of sender-receiver pairs when the source (or destination) is inside (or outside) the clique. clique-clique transfers are faster than other combinations (MIT).

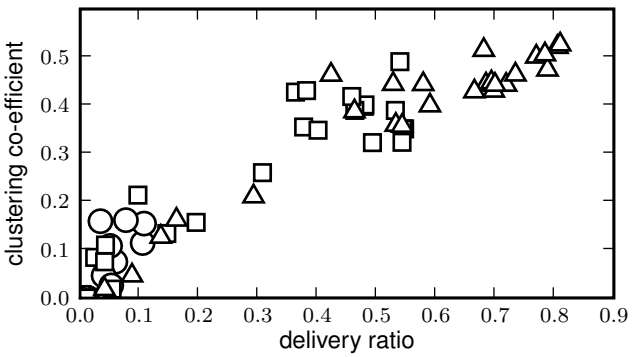

Fig. 9. Scatter plot showing the correlation between delivery ratio during random time windows of different sizes and the clustering coefficient of the *contact* graph for that time window. Squares, circles and triangles represent windows of one-hour, one-day and 3 days, respectively (MIT trace).

leading to large numbers of paths when data is flooded.

While we expect delivery ratio to be high when the reachability graph has a large clique (implying that there is complete connectivity between a large fraction of nodes), it is rather surprising that the converse is true, viz. whenever the delivery ratio is high, there is a large clique in the reachability graph. To understand the implication, consider as example an arbitrarily chosen 3-day window in the MIT trace, with 77 active nodes, a clique of size 46 and an overall delivery ratio of 0.68. If nodes were equally connected, most nodes should be able to reach $\approx 68\%$ of the other nodes during this time window. The clique implies that a subset of 46 nodes ($\approx 60\%$ of the nodes) actually have 100% reachability amongst themselves. The 31 nodes outside the clique form $31 * 30$ source-destination pairs, of which only 59% have paths between them. The table below details the skewed reachability between these classes:

From\To:	**clique**	**outside**
clique	100.00%	78.61%
outside	76.44%	59.35%

In the same window as above, Fig. 8 looks at the quality of the paths between nodes in the clique, outside the clique, as well as the paths that go from source nodes in the clique to destinations outside it, and vice-versa. Plotting the cumulative distribution functions of the delivery times of the quickest paths for each category shows that data is transferred faster when both the sender and receiver are members of the large clique.

Thus, during time intervals when there is a large clique in the reachability graph, the PSN is very successful, but only for the subset of nodes in the maximum clique observed. It is hard to predict the nodes involved because clique membership changes significantly (an average of 33 nodes are added or deleted over successive windows). Clique sizes also vary widely, with a mean size of 28.8, and a standard deviation of 18.2.

3.2 Clustering coefficient predicts delivery ratio

The clique occurs in the *reachability* graph, and cannot be easily detected without flooding all paths and performing extensive computation. We now show that the "cliquishness" of the *contact graph* can serve as an approximation.

Suppose a vertex v has neighbours $\mathcal{N}(v)$, with $|\mathcal{N}(v)| = k_v$. At most $k_v(k_v-1)/2$ edges can exist between them (this occurs when v is part of a k_v-clique). The clustering coefficient [8] of the vertex, C_v, is defined as the fraction of these edges that actually exist. The clustering coefficient of the graph is defined as the average clustering coefficient of all the vertices in the graph. In friendship networks, C_v measures the extent to which friends of v are friends of each other, and hence, approximates the *cliquishness* of the graph.

Fig. 9 shows that the average clustering coefficient of the contact graph correlates well with the delivery ratio achieved during time windows of various sizes. In practice, a node can compute its current clustering coefficient by obtaining a list of recent contacts from each node it meets. The average clustering coefficient of the network can be approximated by propagating current local estimates, for example, by adapting a distributed algorithm to compute aggregates, such as [9].

By using clustering coefficient as a predictor for delivery ratio, senders (or other nodes on their behalf) can make informed decisions about how to deliver data. For instance, a node which observes a low clustering coefficient can aggressively send multiple copies, resend the same data over time, or even bypass the PSN entirely and use a more expensive infrastructure-based communication mechanism such as a satellite connection.

4 Understanding Path Delays

We move from considering the fraction of data delivered to the time taken to deliver data. This section focuses

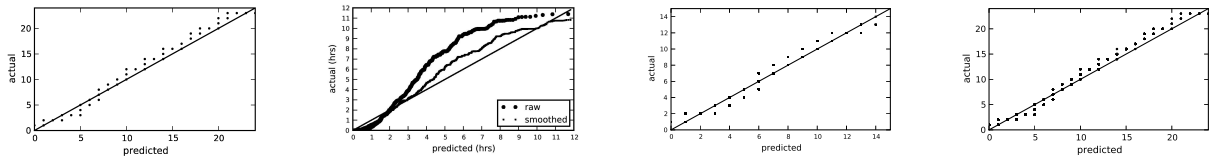

(a) Delivery time: Roughly exponential (MIT, 3 day window)

(b) Hop Delay: Roughly exponential (UCSD, 12 hr window)

(c) No. of hops: Poisson (MIT, one week window)

(d) No. of paths (also degree): Neg. Binomial (UCSD, 6 hr window)

Fig. 10. Distributions related to successful paths. Each Q-Q plot shows fit through correspondence between sample deviates generated according to the theoretical distribution (predicted) and empirical (actual) values. Closeness to predicted=actual diagonal indicates better fit. Different combinations of trace and time window sizes are used to show generality of fit.

H	Hop delay, or time to next hop. Time until a path expands by one more node. $H \sim Exp(rate = \nu)$
N	Number of edges per path. $N \sim Poisson(mean = \lambda)$
L	Number of paths between a random src-dest pair (also node degree). $L \sim NegBin(mean = \eta, dispersion = \theta)$
D	Path delay for a random path
D^*	Delivery time (minimum path delay across all paths between a randomly chosen source & destination)
$G_X(s)$	Probability-generating function of X
$M_X(s)$	Moment-generating function of X. $M_X(s) = G_X(e^X)$

TABLE 1
Summary of notation used to characterise components of path delay and delivery times

on understanding the delays on unicast paths that form during a fixed time window. Paths are discovered by flooding data from every sender to every destination, as described in Sec. 1.

In our method of flooding, every non-destination node (including the source) forwards data to each non-destination node it meets that does not yet have a copy of the data, but receives a data item at most once. The destination node accepts all copies it gets, but does not forward the data further. Note that this does not uncover all the paths that form over time in the contact graph. Rather, since each non-destination node receives data at most once, a tree of paths, rooted at the source, forms over time. We call this the "flood-tree".

First, we examine the quickest paths. Then, we obtain an expression for path delay on any path discovered by flooding, in terms of the delay per hop and number of hops. Finally, we look at the distribution of the number of paths between all possible source-destination pairs. The ultimate goal is to obtain an approximate expression for delivery time, as the minimum of the path delays of a random number of paths.

4.1 Delivery time: path delay on the quickest path

Delivery time is the time taken by the first path to reach the destination. Hence, it is the minimum of the path delays along all paths connecting the source and destination over time. Although there is a huge difference in the path delays of the first (quickest) and the last (slowest) paths that form during a time window, the Quantile-Quantile plot in Fig. 10a shows that delivery time distribution for the quickest paths is almost exponential. Thus, most source-destination pairs have quick paths.

[10], [11] derive analytical expressions which are similar in spirit. However, these assume a constant (averaged) contact rate, whereas the contact rates in our empirical traces are highly heterogeneous (see Sec. 2). Plugging in the average contact rate from the empirical traces into those expressions yields bad fits. Appendix A extends Sec. 4.2 and derives Chernoff bounds for the delivery times.

4.2 Characterising path delays

Next, we examine all successful paths, and express path delay in terms of the delay per hop and number of hops.

4.2.1 Hop delay (H)

The hop delay distribution captures the time that elapses between successive hops on the same path. Fig. 10b shows that the UCSD curve can be fitted to an exponential distribution with rate $\nu \approx 0.0001$, giving a mean time of 2.6 hours to next hop. A similar fit can be obtained for the MIT curve.

For both the MIT and UCSD traces, the fit for the entire curve is approximate ("raw", in Fig. 10b), with goodness of fit varying between different time windows. The fit can be improved by removing outlier values which are likely an artifact of the data set ("smoothed" in Fig. 10b). While the fit is not exact in many windows, we will assume that H is exponential, to simplify the analysis in the following section. This does not limit the applicability of our analysis. We will later show that the key results of Sec. 5 will apply equally for any other distribution which has a moment-generating function.

Note that there is no conflict between the nearly exponential distribution of hop delays and the previously reported power laws (with exponential tails) for inter-contact time distribution [12], [13]. Inter-contact time is

the time between repeated meetings of the same pair of nodes, whereas hop delay measures the time taken by the flooding process: from the time a node receives some data to the time it meets a new node that does not already have a copy of the data. The longer the duration a node carries the data, the greater the chance that data has already been flooded to the nodes it meets. Because of flooding, the hop delay distribution decays rapidly, unlike the inter-contact time distribution.

4.2.2 Number of hops (N)

Several factors work together to limit the number of hops in a successful path. First, we only consider paths that form during a fixed time window. Second, the small-world nature of the human contact graph makes for short paths to a destination; and paths are frozen at the destination because the destination does not forward data further. Third, each node can join the flood-tree at most once. As the tree grows, the number of nodes available to grow the tree and extend a path decrease. Thus extremely long paths are rare. Fig. 10c shows that the number of hops in paths that reach the destination during a one week time window of the MIT trace closely follows a Poisson distribution (The mean number of hops is $\lambda = 5.58$ in this window, and has been found to vary between 5–6 in different windows tested.). A similar fit can be obtained for the UCSD trace.

4.2.3 Path delay (D)

From the above empirically found distributions, we can derive the distribution of the path delay D on a random path as the sum of N hop delays. Thus, D can be written in terms of its moment-generating function (see Table 1 for notation and a summary of the component distributions):

$$M_D(s) = G_N(M_H(s)) = e^{\lambda(\frac{\nu}{\nu - s} - 1)} \tag{1}$$

The average path delay is simply $M'_D(0) = \lambda\nu^{-1}$. Applying a Chernoff-type bound,

$$P\left[D \geq t\right] \leq \min_{s>0} e^{-st} M_D(s) = \min_{s>0} e^{\lambda(\frac{\nu}{\nu - s} - 1) - st} \tag{2}$$

Minimizing by setting $s = \nu - \sqrt{\lambda\nu/t}$, we get (for $t < \sqrt{\lambda/\nu}$)

$$P\left[D \geq t\right] \leq e^{-(\sqrt{\nu t} - \sqrt{\lambda})^2} \tag{3}$$

Remark 1: The form of (3) indicates that the path delay on a random path is also close-to-exponentially distributed.

4.3 Characterising the number of paths (L)

Since each node joins the flood-tree at most once, there can be at most $N-1$ nodes (nodes other than destination) on the tree. Therefore there can be at most $N-1$ paths reaching a destination during the time window.

The actual number of paths depends on the number of unique nodes met by the destination: If the PSN is well mixed and the window is long enough, eventually all intermediate nodes become reachable from the source and get attached to the flood-tree. Thus the number of paths to a destination is determined by the number of distinct neighbours met by the destination over the time window.

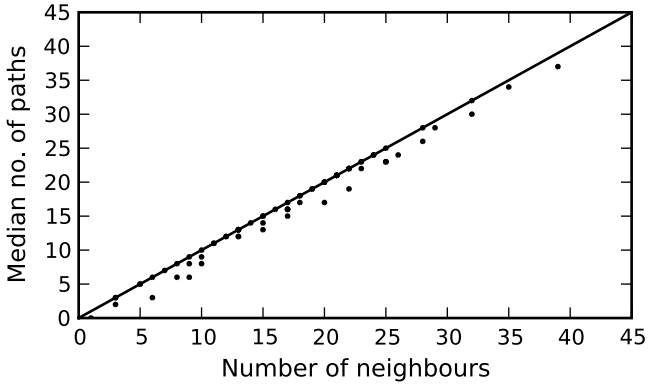

Fig. 11. Median number of successful paths reaching a destination node correlates with the number of distinct neighbours it has. Diagonal shows x axis=y axis. (MIT, one week window)

Fig. 11 empirically confirms this argument, by showing that the median (mean can also be used, instead) number of paths reaching a destination correlates with the number of distinct neighbours it has. As a consequence of this "eventual reachability" phenomenon, the distribution of the number of paths to a destination is simply given by the degree distribution of the who-met-whom graph of the PSN, taken over the entire time window.

Fig. 10d shows that the degree distribution (and the number of paths) in the UCSD trace fits a negative binomial distribution. A similar fit can be obtained for the MIT trace.

The fact that the number of group members that an individual has contact with (the number of neighbours seen) follows the same distribution in both the traces, across time windows of different sizes suggests the possibility of an underlying stochastic mechanism.

The negative binomial is a versatile distribution that can arise in a number of ways [14]. One possible way the negative binomial arises is as a continuous mixture of Poisson distributions where the mixing distribution of the Poisson rate is a gamma distribution. The model assumes that people acquire *new* neighbours according to a Poisson process with rate λ_p. Heterogeneity in the population is modeled by drawing λ_p from some population distribution $P(\lambda_p)$. If $P(\cdot)$ follows the gamma distribution

$$P(\lambda_p = \lambda) = \frac{e^{-(\lambda/\eta_1)}(\lambda/\eta_1)^{(\eta_2 - 1)}}{\eta_1 \Gamma(\eta_2)},$$

then the observed distribution of the number of neighbours seen by individuals in the group would fit the

negative binomial distribution. One interpretation [15] of this is that people acquire new neighbours by searching for people satisfying some personal criterion. People continue to acquire new neighbours until they have η_2 partners. Each potential new partner satisfies the search criterion independently with a probability p_c, which defines the scale parameter $\eta_1 = (1 - p_c)/p_c$.

5 Evaluating the effect of failures

Many studies on Pocket Switched Networks, including ours, implicitly assume that every contact on any path which occurs can be used to successfully transfer data. In reality, many factors could prevent a path from being useful: An intermediate node may run out of storage; the time available during a contact opportunity may not be sufficient; or a node can simply fail.

Since only one path between every source-destination pair needs to succeed for data delivery, individual path failures do not greatly impact the delivery ratio achieved at the end of a time window (unless all paths between a source-destination pair fail, disconnecting the network). However, it can affect the rate at which the delivery ratio evolves: Suppose the quickest path between a pair of nodes would have arrived at t_1, but cannot be used because of a failure. If the first usable path connects the nodes at time $t_2 > t_1$, then between t_2 and t_1 the fraction of data delivered is decreased on account of the path failure. In other words, there is a delay in data delivery, which temporarily shifts the cumulative distribution of delivery times to the right.

Given a sequence of contacts, flooding achieves the best possible delivery times by exploring *every* contact opportunity and thereby finding the path with the *minimum* path delay. This section looks at the degradation in the delivery time distribution when not all of the paths found by flooding can be explored.

Specifically, we study two failure modes: The first, proportional flooding, explores a fixed fraction μ of the paths found by flooding between each source and destination. We show that a constant increase in the fraction of paths explored brings the delivery time distribution of proportional flooding exponentially closer to that of flooding over all paths. The second failure mode, k-copy flooding, explores no more than a fixed number $k > 1$ of the paths found by flooding between each source and destination. Again, a constant increase in k brings the delivery time distribution exponentially close to the optimal delivery time distribution of flooding all paths. Empirically, even small values of k (e.g., $k = 2$ or $k = 5$) closely approximate delivery times found by flooding.

The results of this section imply that the human contact network is remarkably resilient to path failures and the delivery ratio evolves at a close-to-optimal rate even when the majority of paths fail and only a small fraction or a small, bounded number of paths can transport data to the destination. Note that we only admit paths from the original flood-tree, and do not include new paths that repair failures by joining the affected nodes to the flood tree at later contacts. Thus our results in fact underestimate the resilience of the network.

The success of k-copy flooding can provide a loose motivation for routing algorithms that use multiple paths between each sender and destination pair since this could obtain a close-to-optimal delivery time distribution. However, heuristics-based routing algorithms may not find the same paths as found by flooding. Thus, the correspondence is not exact.

5.1 Proportional Flooding

Consider an arbitrary source-destination pair. We will model the path delays between them as being chosen independently and identically from the distribution in (1). Suppose copies of the data are sent along l randomly chosen paths between them. The obtained delivery time D_l^* is the *minimum* of the path delays across all l paths. Using (3) we can write

$$P\left[D_l^* \leq t\right] = 1 - \prod_{i=1}^{l} P\left[D \geq t\right] \geq 1 - e^{-l(\sqrt{\nu t} - \sqrt{\lambda})^2} \quad (4)$$

Note that the above assumes that the l path delays are independent. In reality, paths found by flooding all fan out from a single source node, and the first few hops, close to the source, are typically shared with other paths, violating the independence assumption. Therefore, the model in this section is to be considered only as a simple formulation designed to gain insight into proportional flooding. It is worth mentioning however that in the empirical data sets, we frequently find that the major component of path delay is contributed by the part of the paths closest to the destination, which are not shared with other paths. Also, in the case when only a few paths on flood-tree are being randomly sampled, the number of hops shared is limited.

Consider source-destination pairs with $L = m$ paths connecting them. Full flooding finds the quickest of all m paths and obtains a delivery time distribution $P\left[D_L^* \leq t | L = m\right]$. Proportional flooding chooses a fraction μ of them. From (4), the difference $\Delta(t; \mu)$, in the delivery time distributions between full and proportional flooding, is upper bounded by

$$\Delta(t;\mu) \leq P\left[D_L^* \leq t | L = m\right] - 1 + \ e^{-\mu m\left(\sqrt{\nu t} - \sqrt{\lambda}\right)^2} \quad (5)$$

Remark 2: A constant increase in μ has an exponential effect on Δ: For any t, if μ is increased by some constant, the fraction of data delivered by proportional flooding during $[0, t]$ becomes exponentially closer to that delivered by full flooding. Thus, proportional flooding quickly becomes very effective as μ is increased.

While the above is not unexpected given the model and the resulting distributions as obtained in Sec. 4.2, this observation can be generalised: For a hop delay distribution with moment-generating function $M_H(s)$, (1)–(5) can be rederived to get

$$\Delta(t;\mu) \leq P\left[D_L^* \leq t | L = m\right] - 1 + \exp(\mu m F_H(t)), \quad (6)$$

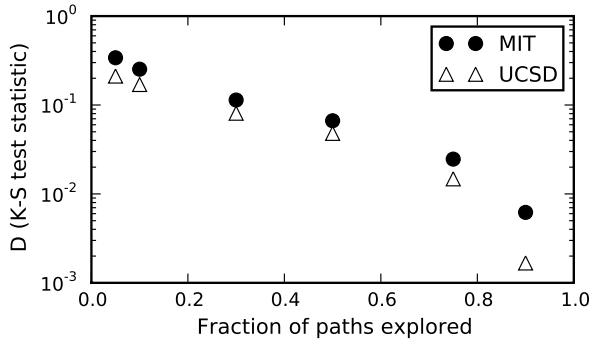

Fig. 12. K-S statistic (D) measuring the difference between the delivery time distributions of full flooding and proportional flooding for different μ. X-axis is linear, Y-axis is log-scale.

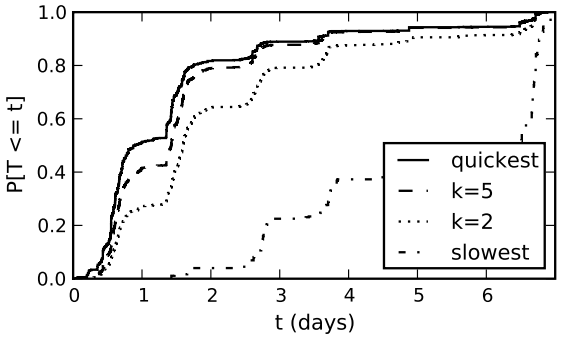

Fig. 13. k-copy flooding: Nodes are connected by multiple paths with different delays (CDFs of the *quickest* and *slowest* are shown). Yet, randomly choosing at most k of the paths to each destination closely approximates the quickest, even for small k. (MIT trace, one week window)

where $F_H(t) = \lambda M_H(s_{\min}(t)) - s_{\min}(t)t - \lambda$ and $s_{\min}(t)$ minimises s in (2)[5]. Thus the exponential decrease in Δ with a constant increase in μ is obtained as long as $F_H(t) < 0$. In other words, our results hold when there are a Poisson number of hops in paths formed over fixed time windows, for any hop delay distribution H that has a moment generating function and satisfies $F_H(t) < 0$.

Also, since

$$\frac{\partial \Delta}{\partial \mu} = mF_H(t)e^{\mu m F_H(t)} < 0,$$

Δ decreases when μ is increased. Furthermore, the rate of decrease is higher for smaller μ – increasing μ from $\mu = 0.1$ to $\mu = 0.2$ results in a greater decrease than an increase from $\mu = 0.6$ to $\mu = 0.7$.

Fig. 12 empirically shows the difference between $D^*(t)$, the delivery time distribution obtained by flooding over all paths, and $D^*_\mu(t)$, the delivery time distribution for proportional flooding using a randomly selected fraction μ of paths between every source and destination. The difference is measured using the Kolmogorov-Smirnov statistic given by $D = \max_t (D^*(t) - D^*_\mu(t))$. Note that the Y-axis is log scale; a constant increase in μ shows an exponential decrease in D.

5.2 From proportional to bounded number of paths

Sec. 4.3 showed that the number of paths to a destination (L), is a random variable that is well modeled by the negative binomial, a positively (or right) skewed distribution. Thus a majority of sender-destination pairs have a small (fewer than average) number of paths, but a minority have a large number of paths, which pulls the average higher. The expected number of paths that need to work for successful proportional flooding is given by $\mu\mathbb{E}[L]$, which is higher than it would be if the minority of node pairs with large numbers of paths were not considered. In the worst case, when there are $(N-1)$ paths between a sender and destination, proportional flooding works only if $\mu(N-1)$ of these are functional.

5. When H is exponentially distributed, we get $F_H(t) = -\left(\sqrt{\nu t} - \sqrt{\lambda}\right)^2$. Plugging this value into (6) yields (5).

This suggests an alternate bounded cost strategy that explores at most a fixed number, k, of the paths between every sender and destination. We call this k-copy flooding. Unlike proportional flooding, k-copy flooding explicitly limits the number of paths explored, and therefore can tolerate a larger number of path failures in the worst case, when there are a large number of paths between a node-pair.

Fig. 13 shows empirically that in our data sets, even for small k ($= 2, 5$), the delivery time distribution of k-copy flooding starts to closely approximate full flooding. To see why, consider the *equivalent fraction* μ_k of paths in proprotional flooding that gives the same expected number of paths as k-copy forwarding:

$$\sum_{l=0}^{k} lP[L=l] + kP[L>k] = \mu_k \mathbb{E}[L] \tag{7}$$

Suppose k is increased by a constant h, resulting in a new equivalent fraction μ_{k+h}. (7) becomes

$$\sum_{l=0}^{k} lP[L=l] + \sum_{j=1}^{h}(k+j)P[L=k+j] + (k+h)P[L>k+h] = \mu_{k+h}\mathbb{E}[L]$$

Regrouping, we get

$$\sum_{l=0}^{k} lP[L=l] + k\left(\sum_{j=1}^{h} P[L=k+j] + P[L>k+h]\right) + \sum_{j=1}^{h} jP[L=k+j] + hP[L>k+h] = \mu_{k+h}\mathbb{E}[L]$$

Comparing with (7), we can write

$$\mu_k \mathbb{E}[L] + \sum_{j=1}^{h} jP[L=k+j] + hP[L>k+h] = \mu_{k+h}\mathbb{E}[L]$$

Thus the *increase* in the equivalent fraction of paths is

$$\mu_{k+h} - \mu_k \geq \frac{h}{\mathbb{E}[L]} \left(\sum_{j=1}^{h} P[L = k+j] + P[L > k+h] \right)$$
$$= h\left(P[L > k]/\mathbb{E}[L]\right) \quad (8)$$

Remark 3: A constant increase in k is equivalent to at least a (scaled) constant increase in the fraction of paths explored by proportional flooding. Thus, as a simple consequence of Remark 2, a constant increase in the number of paths explored in k-copy forwarding moves its delivery time distribution exponentially closer to that of full flooding.

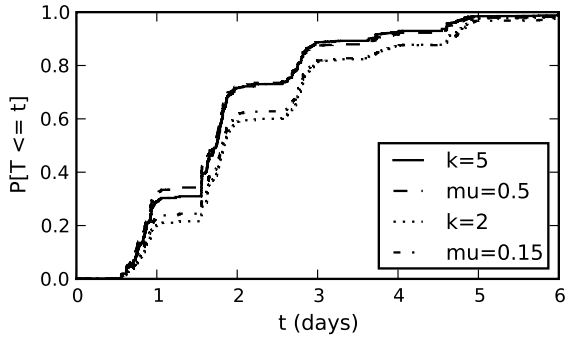

Fig. 14. Proportional flooding with $\mu_2 = 0.15$ of paths has similar delivery times as $k = 2$-copy routing. Similarly $k = 5$ corresponds to $\mu_5 = 0.5$. (MIT, one week window)

This explains why exploring at most a small number k of paths has a delivery time distribution approaching that of flooding over all paths. Fig. 14 empirically shows the equivalent fractions μ_k for the $k = 2$ and $k = 5$ cases discussed previously. Appendix B derives a closed form for μ_k when the number of paths L is negative binomial.

5.3 Resilience and load balancing

The results above suggest that the human contact network is remarkably resilient to path failures and the network's optimal rate of data delivery can still be approximated even when many of the paths do not succeed in delivering data. To conclude, we briefly elucidate this from the perspective of intermediate node failures.

The source and destination rely on the rest of the network to serve as intermediate nodes and form connecting paths. The use of multiple paths provides a degree of resilience against path failures, since only one of the paths needs to succeed. Deterministic strategies that selectively favour particular next hop nodes or even particular paths can potentially overburden certain intermediate nodes that end up getting selected more often, but randomised strategies such as the ones we discuss are more resilient and have fewer bottlenecks.

For any strategy, we can measure the burden placed on a given intermediate node by any given source (respectively, destination) by counting the number of paths of the sender (destination), chosen according to the strategy, in which the node figures as an intermediate hop. We call this number the betweenness centrality of the node for a given source (destination).

Source nodes (destinations) with very few central nodes are vulnerable to being disconnected if the central nodes fail. As Fig. 15 shows, deterministic strategies such as picking the quickest possible path can result in a network that is sparse in central nodes. A randomised strategy results in more central nodes and thus renders the network more resilient against failures. A sender (destination) that has few central nodes is also likely to face congestion if the central nodes hit capacity bottlenecks. The availability of more central nodes opens the possibility of load balancing in such cases.

6 Related Work

Conceptually, PSNs are Delay-Tolerant Networks [16], and generic results from that framework apply. For instance, a forwarding algorithm that has more knowledge about contacts is likely to be more successful [17], and the best performance is achieved by an oracle with knowledge of future contacts.

Nevertheless, the fact that our underlying network is made up of human contacts and is less predictable has a large impact: For instance, reasonably predictable traffic patterns of buses allow a distributed computation of route metrics for packets in vehicular DTNs [17], [18]. Similarly, fixed bus routes allow the use of throwboxes [19] to reliably transfer data between nodes that visit the same location, but at different times.

The variability of PSNs has naturally led to a statistical approach: The inter-contact time distribution of human social contacts has been used to model transmission delay between a randomly chosen source-destination pair [12], [13]. In this work, we take a more macroscopic view and look at the ability of the PSN to simultaneously deliver data between multiple source-destination pairs. This leads us to look at the distribution of the *number* of contacts between randomly chosen source-destination pairs, and find that this distribution is not only crucial for global data delivery performance, but also for the connectivity of the PSN itself.

This paper uses variants of flooding to obtain a better understanding of *achievable* data delivery properties of human contact networks. However, unbounded flooding is expensive. To mitigate this, various routing protocols have been proposed. These typically use various ad-hoc metrics, such as betweenness centrality [20], history of previous meetings [21], and inferred community structure [22]. Computing such metrics can be costly and the computation can be inaccurate due to the high variability inherent in PSNs. Our results point to simpler techniques that could exploit time windows of good connectivity or the use of multiple paths.

[10], [11], [23] model the performance of epidemic routing and its variants. In particular, they derive a closed form for delivery time distribution, and show

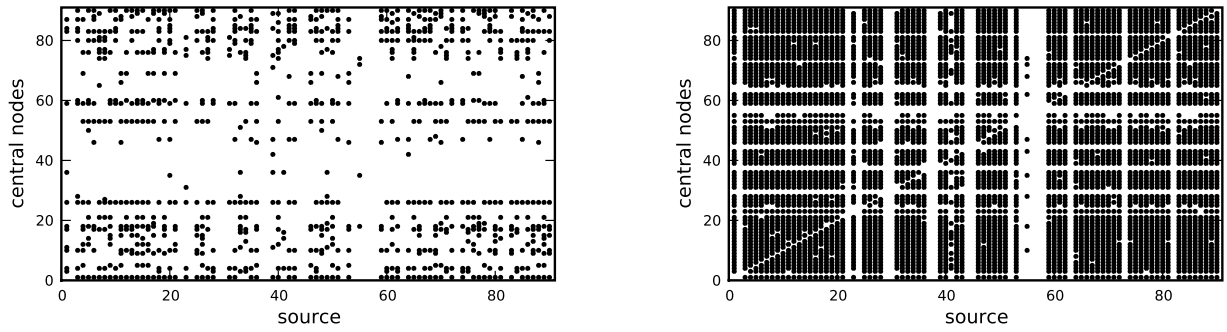

(a) Central nodes on deterministically picked paths

(b) Central nodes on 5 randomly chosen paths

Fig. 15. Scatterplots showing node numbers of source on the X-Axis, and on the Y-Axis, nodes numbers which cross a threshold (=5) betweenness centrality for the corresponding sources. Left figure shows the central nodes when paths are picked according to a deterministic strategy (the quickest path). Right figure shows the central nodes when up to five paths are randomly selected. The random strategy selects more central nodes and spreads the load more evenly. A similar set of figures can be obtained by looking at the most central nodes for a given *destination*. (MIT trace, one week window)

it to be accurate for certain common mobility models. However, several simplifying assumptions are made, including an exponential inter-contact time between node pairs. Unforunately, human contact networks are known to have power law inter-contact times with exponential tails [12], [13]. Furthermore, [10], [11], [23] use a constant contact rate, whereas our studies show that human contacts are highly heterogeneous. [24] considers heterogeneous contact rates between mobile devices but only in the context of establishing an epidemic threshold for virus spread.

The number of paths found by flooding is crucial to the success of proportional and k-copy flooding. Counting differently, [25] reports a phenomenon of "path explosion" wherein thousands of paths reach a destination shortly after the first, many of which are duplicates, shifted in time. In contrast, duplicate paths are prevented in our method of counting, by having nodes remember if they have already received some data, resulting in a maximum of $N-2$ paths between a source and destination.

The power of using multiple paths has been recognised. Binary Spraying, which forms the basis for two schemes (spray and wait, spray and focus) has been shown to be optimal in the simple case when node movement is independent and identically distributed [26]. [27] noted that among routing schemes evaluated, those using more than one copy performed better. Furthermore, all algorithms employing multiple paths showed similar average delivery times. The success of k-copy flooding suggests a possible explanation for this result. Similarly, [28] finds that the delivery ratio achieved by a given time is largely independent of the propensity of nodes to carry other people's data. They suggest the existence of multiple paths as an explanation. At an abstract level, the refusal of a node to carry another node's data can be treated as a path failure. Thus Sec. 5 corroborates [28] and provides a direct explanation.

We mention in passing that our finding of large cliques in the reachability graphs is loosely analogous to the giant strongly connected component in the WWW graph that accounts for most of its short paths [29]. Similarly, our finding that the human contact graph is resilient to path failure is echoed in the attack tolerance demonstrated for static graphs of many complex networks [30].

7 Conclusion

This work examined the data delivery properties of human contact networks using empirical traces of contacts between loosely connected groups of people. The ability to deliver data was measured by the fraction of data delivered by flooding data between every possible source-destination pair.

The effectiveness of the network in delivering data is determined by the contact occurrence distribution and order of occurrence of contacts. The contact occurrence distribution exhibits an interesting dichotomy with many contacts occurring rarely, and a few occurring very frequently. At a macroscopic level, this suggests that delivery of packets is difficult: The connectivity of the network is crucially dependent on rare contacts occurring, and inadequate mixing of data due to repeated occurrences of frequent contacts increases the global count of contacts required for connecting a given fraction of node pairs.

However, different time windows of same duration can achieve significantly different delivery ratios. Successful time windows are a result of unequal connectivity and are characterised by a large clique of nodes that can all reach each other. It was demonstrated that the successful time windows as well as the clique members

can be identified by looking at the clustering co-efficient over the contact graph.

We then examined distributions of random variables that contribute to the delay on paths that successfully connect source nodes to their destinations. Among other results, it was found that the number of hops on a path follows a Poisson distribution. Primarily as a consequence of this, it was shown that the human contact network exhibits a remarkable resilience to random path failures. Increasing the number or fraction of paths explored between source and destination by a constant brings the delivery time distribution exponentially close to the optimal. Thus, the network can continue to deliver data at a near optimal rate even when a large number of random path failures occur.

The results of this work could be used to adopt a principled approach to the development of routing algorithms for Pocket Switched Networks, rather than relying on heuristics as motivation. For instance, one possibility is to exploit periods of good connectivity by computing the current clustering co-efficient. Similarly, randomised sampling amongst paths considered could lead to better resilience and load balancing properties.

APPENDIX A
CHERNOFF BOUNDS FOR DELIVERY TIMES

Using (4), the delivery time distribution D^* of all source destination pairs can be bounded from below by

$$\begin{aligned} P[D^* \leq t] &= \sum_l P[D_l^* \leq t | L = l] P[L = l] \\ &\geq 1 - \mathbb{E}\left[e^{-L(\sqrt{\nu t} - \sqrt{\lambda})^2}\right] \\ &= 1 - M_L\left(-(\sqrt{\nu t} - \sqrt{\lambda})^2\right) \end{aligned} \tag{9}$$

where M_L is the moment generating function of L. Assuming that L is a negative binomial with mean η and dispersion θ,

$$P[D^* \leq t] \geq 1 - \left(\frac{1}{1 + \frac{\eta}{\theta}\left(1 - e^{-\left(\sqrt{\nu t} - \sqrt{\lambda}\right)^2}\right)}\right)^{\theta} \tag{10}$$

Similarly, we can use a Chernoff bound for $P[D \leq t] = P[t - D \geq 0] \leq e^{st} M_D(-s) = e^{-\left(\sqrt{\nu t} - \sqrt{\lambda}\right)^2}$, where $s = \sqrt{\lambda \nu / t} - \nu$ gives the best bound. Substituting for $P[D \geq t] = 1 - P[D \leq t]$ in (4)

$$P[D^* \leq t | L = l] \leq 1 - \left(1 - e^{-(\sqrt{\nu t} - \sqrt{\lambda})^2}\right)^l \tag{11}$$

and performing the same calculations, we obtain a lower bound for D^*.

$$\begin{aligned} P[D^* \leq t] &= \sum_l P[D^* \leq t | L = l] P[L = l] \\ &\leq 1 - \mathbb{E}\left[\left(1 - e^{-(\sqrt{\nu t} - \sqrt{\lambda})^2}\right)^L\right] \\ &= 1 - G_L\left(1 - e^{\left(-(\sqrt{\nu t} - \sqrt{\lambda})^2\right)}\right) \end{aligned} \tag{12}$$

When L is a negative binomial, as above,

$$P[D^* \leq t] \leq 1 - \left(\frac{1}{1 + \frac{\eta}{\theta} e^{-(\sqrt{\nu t} - \sqrt{\lambda})^2}}\right)^{\theta} \tag{13}$$

APPENDIX B
DERIVING AN EQUIVALENT FRACTION μ_k FOR $L \sim$ NEGBIN(η, θ)

This section derives an equivalence between k-copy forwarding and proportional flooding, from the general form (7), when the degree distribution (equivalently, the number of paths to a destination) is $L \sim \text{NegBin}(\text{mean} = \eta, \text{dispersion} = \theta)$. The probability mass function for L can be written as [31]:

$$P[L = l; \eta, \theta] = \frac{\Gamma(\theta + l)}{(l)!\,\Gamma(\theta)} \left(\frac{\theta}{\eta + \theta}\right)^{\theta} \left(\frac{\eta}{\eta + \theta}\right)^{l}$$

First, using $p = \theta/(\eta + \theta)$, we have [31]

$$P[L > k] = 1 - P[L \leq k] = 1 - I_p(\theta, k + 1) \tag{14}$$

where $I_x(a, b) = B(x; a, b)/B(a, b)$ is the regularized incomplete Beta function. Next,

$$\begin{aligned} \sum_{l=0}^{k} l P[L = l] &= \sum_{l=1}^{k} \frac{\Gamma(\theta + l)}{(l-1)!\,\Gamma(\theta)} p^{\theta} (1-p)^l \\ &= \theta \frac{(1-p)}{p} \sum_{l=1}^{k} \frac{\Gamma(\theta + 1 + l - 1)}{(l-1)!\,\Gamma(\theta)} p^{\theta+1} (1-p)^{l-1} \\ &= \theta \frac{(1-p)}{p} \sum_{l'=0}^{k-1} P[L = l'; \eta, \theta + 1] \\ &= \eta I_p(\theta + 1, k) \end{aligned} \tag{15}$$

Substituting (14) and (15) into (7),we get

$$\mu_k = I_p(\theta + 1, k) + \frac{k}{\eta} I_{1-p}(k + 1, \theta) \tag{16}$$

REFERENCES

[1] P. Hui *et al.*, "Pocket switched networks and the consequences of human mobility in conference environments," in *Proceedings of ACM SIGCOMM first workshop on delay tolerant networking and related topics*, 2005.

[2] M. Grossglauser and D. N. C. Tse, "Mobility increases the capacity of ad hoc wireless networks," *IEEE/ACM Trans. Netw.*, vol. 10, no. 4, pp. 477–486, 2002.

[3] J. Travers and S. Milgram, "An experimental study of the small world problem," *Sociometry*, vol. 32, no. 4, pp. 425–443, 1969.

[4] R. I. M. Dunbar, "Co-evolution of neocortex size, group size and language in humans," *Behavioral and Brain Sciences*, vol. 16, 1993.

[5] "UCSD", "Wireless topology discovery project," http://sysnet.ucsd.edu/wtd/wtd.html, 2004.

[6] N. Eagle and A. S. Pentland, "CRAWDAD data set mit/reality (v. 2005-07-01)," http://crawdad.cs.dartmouth.edu/mit/reality.

[7] E. Yoneki, P. Hui, and J. Crowcroft, "Visualizing community detection in opportunistic networks," in *CHANTS'07: Proc. of the second ACM workshop on Challenged Networks*, 2007, pp. 93–96.

[8] D. J. Watts and S. H. Strogatz, "Collective dynamics of 'small-world' networks." *Nature*, vol. 393, no. 6684, pp. 440–442, 1998.

[9] J. Zhao, R. Govindan, and D. Estrin, "Computing aggregates for monitoring wireless sensor networks," in *2003 IEEE International Workshop on Sensor Network Protocols and Applications, 2003. Proceedings of the First IEEE*, 2003, pp. 139–148.

[10] T. Small and Z. J. Haas, "The shared wireless infostation model: a new ad hoc networking paradigm (or where there is a whale, there is a way)," in *MobiHoc*, 2003.

[11] X. Zhang, G. Neglia, J. Kurose, and D. Towsley, "Performance modeling of epidemic routing," *Comput. Netw.*, vol. 51, no. 10, pp. 2867–2891, 2007.

[12] T. Karagiannis, J.-Y. Le Boudec, and M. Vojnovic, "Power law and exponential decay of inter contact times between mobile devices," in *MOBICOM*, 2007.

[13] A. Chaintreau *et al.*, "Impact of human mobility on opportunistic forwarding algorithms," *IEEE Transactions on Mobile Computing*, vol. 6, no. 6, pp. 606–620, June 2007.

[14] M. T. Boswell and G. P. Patil, *Random Counts for Scientific Work*. Pennsylvania State University Press, 1970, vol. 1, ch. Chance Mechanisms Generating the Negative Binomial Distribution.

[15] M. S. Handcock and J. H. Jones, "Interval estimates for epidemic thresholds in two-sex network models," *Theoretical Population Biology*, vol. 70, no. 2, pp. 125 – 134, 2006.

[16] K. Fall, "A delay-tolerant network architecture for challenged internets," in *"SIGCOMM"*, 2003.

[17] S. Jain, K. Fall, and R. Patra, "Routing in a delay tolerant network," in *SIGCOMM*, 2004.

[18] A. Balasubramanian, B. N. Levine, and A. Venkataramani, "DTN Routing as a Resource Allocation Problem," in *SIGCOMM*, 2007.

[19] W. Zhao *et al.*, "Capacity Enhancement using Throwboxes in DTNs," in *Proc. IEEE Intl Conf on Mobile Ad hoc and Sensor Systems (MASS)*, 2006.

[20] E. Daly and M. Haahr, "Social network analysis for routing in disconnected delay-tolerant manets," in *MobiHoc*, 2007.

[21] A. Lindgren, A. Doria, and O. Schelen, "Probabilistic routing in intermittently connected networks," in *Proc. SAPIR Wkshp*, 2004.

[22] P. Hui, J. Crowcroft, and E. Yoneki, "Bubble rap: Social-based forwarding in delay tolerant networks," in *MobiHoc*, 2008.

[23] R. Groenevelt, P. Nain, and G. Koole, "The message delay in mobile ad hoc networks," *Perform. Eval.*, vol. 62, no. 1-4, pp. 210–228, 2005.

[24] J. W. Mickens and B. D. Noble, "Modeling epidemic spreading in mobile environments," in *WiSe '05: Proceedings of the 4th ACM workshop on Wireless security*, 2005.

[25] V. Erramilli, A. Chaintreau, M. Crovella, and C. Diot, "Diversity of forwarding paths in pocket switched networks," in *Proceedings of ACM Internet Measurement Conference*, October 2007.

[26] T. Spyropoulos, K. Psounis, and C. S. Raghavendra, "Efficient routing in intermittently connected mobile networks: the multiple-copy case," *IEEE/ACM Trans. Netw.*, vol. 16, no. 1, 2008.

[27] V. Erramilli, M. Crovella, A. Chaintreau, and C. Diot, "Delegation forwarding," in *MobiHoc*, 2008.

[28] P. Hui, K. Xu, V. Li, J. Crowcroft, V. Latora, and P. Lio, "Selfishness, altruism and message spreading in mobile social networks," in *Proc. of First IEEE International Workshop on Network Science For Communication Networks (NetSciCom09)*, 2009.

[29] A. Broder, R. Kumar, F. Maghoul, P. Raghavan, S. Rajagopalan, R. Stata, A. Tomkins, and J. Wiener, "Graph structure in the web," *Computer Networks*, vol. 33, no. 1-6, pp. 309–320, 2000.

[30] R. Albert, H. Jeong, and A.-L. Barabàsi, "Error and attack tolerance of complex networks," *Nature*, vol. 406, pp. 378–382, 2000.

[31] N. Kotz, A. Kemp, and S. Kotz, *Univariate Discrete Distributions*, 3rd ed. Wiley, 2005.

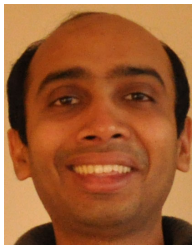

Nishanth Sastry Nishanth Sastry is a PhD student in the Computer Laboratory at the University of Cambridge, where he has been funded by a St. John's Benefactor's Scholarship. Prior to this, he was at IBM for five years, first in the software group and then at IBM Research. He also worked for a year at Cisco Systems. He has a Master's degree in Computer Science from The University of Texas at Austin and a Bachelor's degree (distinction) in Computer Science and Engineering from R.V. College of Engineering, Bangalore University, India. His honours include a Best Undergraduate Project Award, a Best Paper Award from the Computer Society of India, a Cisco Achievement Program Award, a Yunus Innovation Challenge Award at the MIT IDEAS Competition and several awards for his work at IBM. His work has ranged over several layers of the network stack and he is currently involved in building better networked systems by harnessing social network information.

D. Manjunath received his BE from Mysore University, MS from IIT Madras, India and PhD from Rensselaer Polytechnic Inst, Troy NY in 1986, 1989 and 1993 respectively. He has worked in the Corporate R & D Center of GE in Schenectady NY (1990), CIS Dept., University of Delaware (1992-93) and the CS Dept., University of Toronto (1993-94). He was with the Department of Electrical Engineering of IIT Kanpur during 1994-98. He has been with the Electrical Engineering Department of IIT Bombay since July 1998 where he is now a Professor. His research interests are in the general areas of communication networks and performance analysis. His recent research has concentrated on network traffic and performance measurement, analysis of random wireless data and sensor networks, network pricing and queue control. He has won the best paper award in ACM Sigmetrics 2010 and was a Benjamin Meaker Visiting Professor at the University of Bristol during 2010. He is a coauthor of *Communication Networking: An Analytical Approach* (2004) and *Wireless Networking* (2008) both of which are published by Morgan-Kaufman.

Karen Sollins Dr. Karen Sollins is a Principal Scientist at the Massachusetts Institute of Technology, where she also received her graduate degrees. Her research concentrates on Internet scale network architecture, with a current focus on distributed network management. She has published in the areas of security, naming, network architecture, information centric networking, among others. She is Co-Chair of the MIT Communications Futures Program Privacy and Security Working Group, and spent two years as a Senior Program Director at the National Science Foundation. She is a member of both the IEEE and ACM.

Jon Crowcroft is the Marconi Professor of Networked Systems in the Computer Laboratory, of the University of Cambridge. Prior to that he was professor of networked systems at UCL in the Computer Science Department. He has supervised over 45 PhD students and over 150 Masters students.

He is a Fellow of the ACM, a Fellow of the British Computer Society and a Fellow of the IEE and a Fellow of the Royal Academy of Engineering, as well as a Fellow of the IEEE. He was a member of the IAB 96-02, and went to the first 50 IETF meetings; was general chair for the ACM SIGCOMM 95-99; is recipient of Sigcomm Award in 2009. He is the Principle Investigator in the Computer Lab for the EU Social Networks project, the EPSRC funded Horizon Digital Economy project, hubbed at Nottingham, the EPSRC funded project on federated sensor nets project FRESNEL, in collaboration with Oxford; and a new 5-year project towards a Carbon Neutral Internet with Leeds.